

# Fully automated measurement of total adipose tissue volume using quantitative chemical shift MRI: Phantom Validation

A. H. Poonawalla<sup>1</sup>, C. D. Hines<sup>1</sup>, D. Hernando<sup>1</sup>, P. Irarrazaval<sup>1,2</sup>, and S. B. Reeder<sup>1</sup>

<sup>1</sup>Radiology, University of Wisconsin, Madison, WI, United States, <sup>2</sup>Biomedical Engineering, Pontificia Universidad Catolica de Chile, Santiago, Chile

**INTRODUCTION.** Accurate identification and quantification of total adipose tissue (TAT) volume is a key first step for segmentation and measurement of visceral adipose tissue (VAT) and subcutaneous adipose tissue (SCAT), which are critical metrics in diagnosis and treatment of obesity-related diabetes, cardiovascular disease, and metabolic syndrome (1-3). Anthropometric measurements of waist circumference, waist-hip ratio, and body mass index (BMI) are widely used clinically to indirectly characterize TAT, VAT and SCAT, but are highly prone to systematic error (4-5) and correlate poorly with actual adipose tissue volumes (6-7). Qualitative segmentation using empirical signal thresholds and manual segmentation of adipose tissue on T1-weighted MRI is considered the reference standard for direct VAT measurement, but is prohibitively time-consuming for clinical use. Qualitative manual segmentation is also subject to partial volume effects at fat-water and fat-void interfaces, potentially leading to significant errors and poor repeatability in TAT/VAT/SCAT estimation. Chemical shift-based fat/water MRI methods are more accurate than T1-weighted MRI for visualizing adipose tissue (8-9) and potentially permit more rapid adipose tissue segmentation (10-11) by applying a simple fat-fraction threshold. However, the quantitative accuracy of chemical shift methods is confounded by relaxation effects (12-14) and spectral complexity of fat (13, 15), resulting in significant errors in fat-fraction values (16-17). Also, to avoid partial volume effects at signal boundaries, the fat-fraction threshold for adipose tissue is typically defined as 50%, implicitly assuming a maximum fat fraction ( $\eta_{MAX}$ ) of 100%, but in vivo adipose tissue also contains organelles, blood vessels, and water components which result in a true  $\eta_{MAX} < 100\%$ . Therefore,  $\eta_{MAX}/2$  is a more physiologically meaningful choice for adipose tissue thresholding, which can be directly measured from quantitative fat-fraction maps. **The purpose of this work** is to describe a quantitative chemical shift-based fat/water MRI method for fully automated estimation of  $\eta_{MAX}$  and volume of TAT. To assess the robustness of the TAT volume measurement with respect to partial volume effects, we employ a series of oil phantoms with varying volume and surface area complexity, using agar gel, glass rods, and empty plastic vials.

**METHODS.** A phantom comprised of nine bottles of peanut oil, with varying oil volumes (250 cc, 500 cc, and 750 cc) and increasing surface area complexity (oil, oil with 2% agar spheres, and oil with 2% agar spheres, glass rods, and air cavities) was constructed to test the performance of the TAT estimation algorithm (Figure 1). MR images were acquired on a clinical 3.0 T MRI scanner (GE Healthcare, Waukesha WI) using a 32-channel phased-array body coil (Neocoil, Pewaukee WI). The acquisition used a single-slab 3D multi-echo spoiled gradient-echo (SPGR) pulse sequence (18) with 6 echoes/TR and 1.2 ms echo spacing (13, 15), and flip angle of  $3^\circ$  to minimize T1-weighting bias (12). Data was acquired in the sagittal plane with 44.8 cm FOV, 148 x 148 matrix and 160 slices of 2 mm, interpolated to 1.75 x 1.75 x 1.0 mm<sup>3</sup>. Auto-calibrated parallel imaging (ARC) (19) accelerated the acquisition by a factor of 5.32, for total scan time of 26 sec. Fat and water images were reconstructed offline and used to generate quantitative fat-fraction maps with full dynamic range of 0-100% (12). A custom thresholding algorithm was then applied to fat and water data to automatically suppress background noise and signal voids from glass and air cavities. The maximum fat-fraction value  $\eta_{MAX}$  was estimated using histogram analysis, with identical value in all bottles of the noise-masked fat-fraction map with values greater than or equal to  $\eta_{MAX}/2$ . The TAT volume was then obtained by multiplying the number of voxels in the adipose tissue mask by the single-voxel volume. Total processing time of raw fat and water data to TAT volume was < 5 min and required no user intervention.

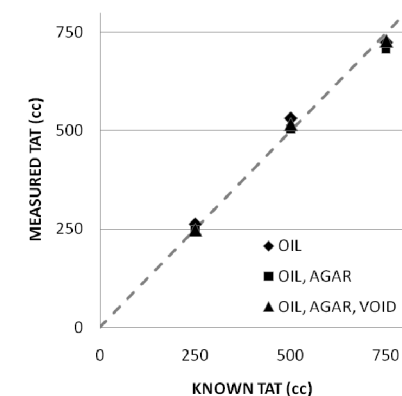


**FIGURE 2.** The TAT volumes measured by the fully automatic algorithm are highly accurate, and robust despite increasing partial volume effects;  $r^2 = 0.991, 0.995,$  and  $0.996$  for OIL, OIL+AGAR, and OIL+AGAR+VOID, respectively.

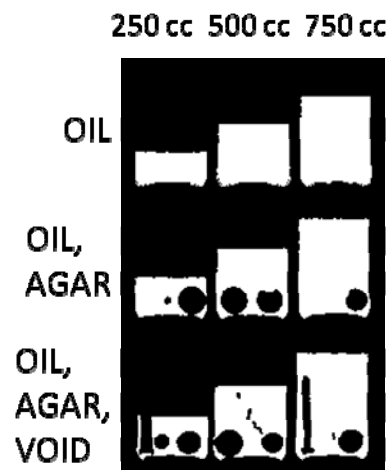


**FIGURE 1.** Noise-masked fat-fraction maps for each oil phantom of varying volume and surface area complexity. The fat-fraction values are nearly unity in oil and nearly zero in agar and the signal void regions of air and glass.

**RESULTS.** The automated algorithm accurately measured TAT volume in each phantom, with maximum error under 3% of the known volume of oil ( $p > 0.44$ ). The accuracy of the algorithm was unaffected by increasing surface area of fat-water and fat-void boundaries (Figure 2).

**DISCUSSION.** The automated TAT algorithm was immune to partial volume effects, providing highly accurate measurements of TAT even at the higher levels of surface area complexity.

**REFERENCES.** [1] Alberti KG, Lancet. 2005;366:1059. [2] Bergman RN, Obesity. 2006;14:16S. [3] Despres JP, Nature. 2006;444:881. [4] Agarwal SK, Obesity. 2009;17:1056. [5] Mason C, Obesity. 2009;17:1789. [6] Joy T, Metabolism. 2009;58:828. [7] Ludescher B, Invest Radiol. 2009;44:712. [8] Bley TA, JMRI. 2010;31:4. [9] Bornert P, JMRI. 2007;25:660. [10] Alabousi A. Proc ISMRM. 2009;17:2880. [11] Kullberg J, JMRI. 2009;30:185. [12] Liu CY, MRM. 2007;58:354. [13] Yu H, JMRI. 2007;26:1153. [14] Bydder M, MRI. 2008;26:347. [15] Yu H, MRM. 2008;60:1122. [16] Kim H, MRM. 2008;59:521. [17] Reeder SB, JMRI. 2009;29:1332. [18] Reeder SB, JMRI. 2007;25:644. [19] Brau AC, MRM. 2008;59:382.

**Acknowledgments:** This work was supported by the NIH (R01 DK083380, R01 DK088925 and RC1 EB010384), the Coulter Foundation, and GE Healthcare.